High-Efficiency Current-Source Converter for All-Electric Wave Energy Conversion Systems

S.P.McDonald [#1], V.Pickert [#2], N.Baker[#3]

[#] *School of Electrical and Electronic Engineering, Newcastle University*

Merz Court, Newcastle upon Tyne, NE1 7RU, UK.

[1] steve.mcdonald@newcastle.ac.uk

[2] volker.pickert@newcastle.ac.uk

[3] nick.baker@newcastle.ac.uk

Abstract—**Power Take-Off (PTO) for Wave Energy Converters (WECs) is a challenge for developers.**

Typically a mechanical PTO involves hydraulics, compressed air or gears to convert the high force, low velocity energy flux from the WEC into a high velocity, low force form suitable for electrical generation. A conventional generator is used, simplifying the Electrical Power Conversion System (EPCS). Further, the mechanical PTO solution permits the storage of energy to reduce the naturally peaky nature of the WEC power flow or tune the resonant frequency of the WEC.

The E-Drive project aims to develop a direct-drive PTO to convert mechanical energy from the WEC directly into electrical energy suitable for export.

The EPCS needs to be designed for the time varying nature of the WEC power flow and to control the WEC. For example, to provide WEC reactive power control. The EPCS is modular to improve reliability and adopts a Current Source Converter (CSC) as the generator interface with localised energy storage and a multilevel inverter as the grid interface. This paper discusses the suitability of the CSC and explores reactive power control for a case study WEC. Results from the WEC model with the generator and CSC are presented.

Keywords— **Marine technology, Wave power, Power electronics, Current-source, Energy conversion, Direct drive.**

I. Introduction

The E-drive project is investigating new solutions to a fundamental challenge for existing Wave Energy Converters (WECs), namely the reliability and complexity of the electro-mechanical Power Take off (PTO). One of the major characteristics of any WEC is the periodic nature and dynamic range of the energy source, i.e. the waves [1]. When coupled with the challenges involved in successfully controlling a WEC for optimal energy capture in a range of sea-states, it is clear that designing a direct-drive PTO is non-trivial [2].

In a conventional PTO, mechanical components convert energy from the WEC into a form more suited to electrical generation which is typically achieved via a conventional high speed electrical machine. This simplifies the Electrical Power Conversion System (EPCS) within the PTO. The mechanical system's ability to store energy within springs, compressed air or hydraulic accumulators reduces the peaky nature of the power flow through the EPCS. This storage capability enables reactive control of the WEC for optimal energy extraction. These features tend to underpin the argument for an electro-mechanical PTO approach [3].

The electromechanical PTO is not without its drawbacks such as wear of moving parts. The main objective of the E-Drive project is to develop an integrated low-speed direct-drive PTO. This will convert the low-speed high-torque motion from the WEC directly into electrical energy suitable for feeding into the utility. The reduction in mechanical complexity of the PTO and improved reliability are two potential advantages of this approach. Inevitably direct-drive places significant additional demands on the EPCS and this is the focus of this particular investigation.

Defining the functional requirements for a WEC PTO and in particular for the E-Drive case study is not straightforward. The range of variables in any WEC design include: wave resource, location, device type, structure, mooring, PTO components and control methodology. To overcome this issue a generic point absorber WEC, operating in simple sea-states which are typical of those found off the west coast of Scotland, is used as a case study enabling analysis of the direct-drive PTO concept.

The evolution of a time domain point absorber WEC model is described. This model is used to provide insight into the forces and dimensions for the proposed PTO components and give some confidence in the capability of a basic control approach. The findings could then be optimised to suit a specific WEC or application using more sophisticated modelling and control techniques. Subsequently, the concept of a generator interface based on a Current Source Converter (CSC) is described. The CSC is designed to operate with a modular linear generator being developed within the same project [4, 5].

This paper is organised as follows: The basic concept for the E-drive PTO is presented in section II outlining the main function blocks and justifying the adoption of a CSC generator interface, the detail of which is covered in Section III. Section IV describes the development of a WEC model which is then used to derive a functional specification for the operation of the CSC. Results are provided in Section V. Finally, discussion and conclusions are presented within sections VI and VII.

II. The E-Drive PTO concept

The purpose of the EPCS is to convert the mechanical power extracted from the WEC for transmission to the nearest electricity grid connection point. This connection point may be several kilometres from the WEC, necessitating medium voltage transmission, i.e. 11kV. An intermediate offshore substation might be useful in an array, with the added benefit of enabling power sharing between the WECs [6]. In such an array configuration, power levelling, inter-device protection and array fault tolerance are further features that would be considered at the design stage. However in a single WEC solution, which is what we are assuming here, the EPCS needs to be capable of delivering acceptable power quality to the grid or offshore substation independently. Further, fault-ride-through will typically be a requirement imposed by the grid operator to support network stability [7]. Thus, in a direct-drive solution, it is recognised that a local Energy Storage System (ESS) will be required and supercapacitors are considered the most likely candidate to achieve this, although the technology is still evolving [8, 9]. The needs of the automotive industry and others are constantly driving storage technology in terms of cost, capacity and reliability such that it is likely to be viable for use in wave energy applications in the near future.

Conventionally the EPCS components for a WEC are based on an industrial variable-speed-drive configuration similar to that illustrated in Fig. 1. A generator charges a DC-link capacitor via a Voltage Source Converter (VSC) or rectifier and then a Voltage Source Inverter (VSI) is used to convert the DC-link voltage and current into grid frequency AC voltages and currents.

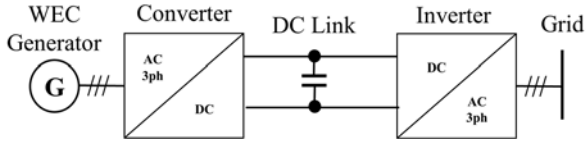

Fig. 1. VSD block diagram

For an application with modest speed variation requirements this arrangement works well and the various components can be optimally selected. For the E-Drive EPCS the following features are required:

- Variable-speed operation; the generator will be accelerating from zero to full speed and back to zero every few seconds.
- Enhanced reliability and fault tolerance – failure of one or more PTO components should not prevent the WEC from operating, albeit at reduced output capacity.
- Four-quadrant operation – for reactive power control of the WEC four-quadrant operation is required.
- Local energy storage – reactive power control requires significant power flows over and above the average power being fed into the grid [10].

The conversion of the relatively slow mechanical buoy motion into useful electrical energy using linear machines and magnetic gearing is the subject of ongoing investigation within the project [5]. The generator interface is necessarily generic at this stage and will be adapted for the specific voltage, current and frequency ratings of the final machine design in due course.

A simplified block schematic of the proposed E-drive PTO is shown in Fig. 2. The idea is that the linear generator is made up of a number of identical 3-phase segments, each with its own PTO subsection. Three PTO subsections are shown here. Within each PTO subsection there is a CSC generator interface, an ESS and a Grid Interface Modules (GIM). The GIMs are recombined to form the overall grid interface. One option under consideration is to adopt a Modular Multilevel Inverter (MMI) topology for the grid interface. Provided enough PTO subsections are in service at any one time, the MMI will be able to continue to deliver power, albeit at a reduced capacity [11]. Galvanic isolation between each of the PTO subsections is required but not shown.

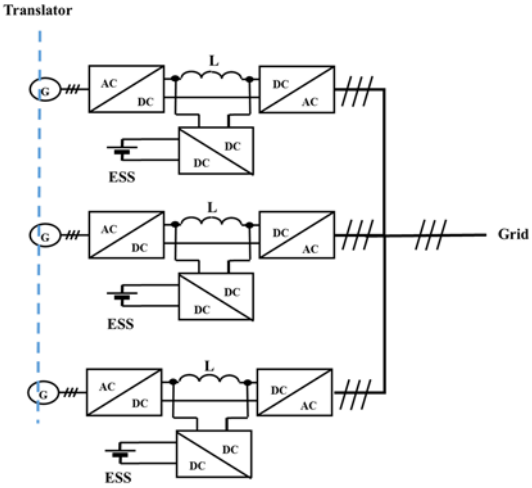

Fig. 2. E-Drive PTO block diagram

III. CSC generator interface

Whilst the VSC and VSI combination can be used for this application, the selection of optimal components becomes more challenging. The DC-link voltage is defined by the grid voltage resulting in reduced device utilisation on the VSC. Typically, an additional DC/DC conversion stage is required to match the generator output to the required DC-link voltage. The DC-link capacitors, in particular aluminium electrolytic devices, are considered to be a significant source of failures, especially when subject to high ripple currents [12]. A CSC should be more suited as a WEC generator interface because the DC-Link component is an inductor which is relatively robust and better able to cope with the power flux. The relatively poor dynamic performance, typically quoted as a drawback of the CSC, is unlikely to be an issue as typical WEC time constants are several seconds. The reduced dv/dt in the output and short-circuit current limiting for the switches are also advantages.

A three-phase CSC model has been developed in PLECS® using Reverse-Blocking Insulated Gate Bipolar Transistors (RB-IGBT's) and Space-Vector (SV) modulation techniques [13, 14]. The advantage of using RB-IGBTs is reduced on-state losses compared to using a separate diode and conventional IGBT whilst still enabling reasonable switching frequencies of

a few kHz. The SV modulation approach minimises switching transitions. Control of the CSC ensures the current in each phase is either in-phase (motoring) or 180 degrees out of phase (generating) with the back-emf of the generator as required for the Vernier Hybrid Linear Machine (VHLM) being used as a basis for this evaluation. The phase current magnitude is controlled by adjusting the DC-Link current to suit the loading requirement of the generator and the modulation index is kept at 100 percent, maximising the CSC efficiency. The purpose of this model is to ensure the magnitude of the CSC variables are reasonable for the proposed generator designs and WEC. The generator is designed for an output of 50A pk. Figure 3 shows that the CSC current and voltage waveforms to the generator are not distorted and in Fig. 5 the DC-Link current ripple is limited to 2.5Arms, the AC output filter capacitors are 20µF and the DC-link inductor is 0.1mH. At 200% rated load, i.e. 100Apk the RB-IGBT device voltage limits are likely to be exceeded, Fig. 6.

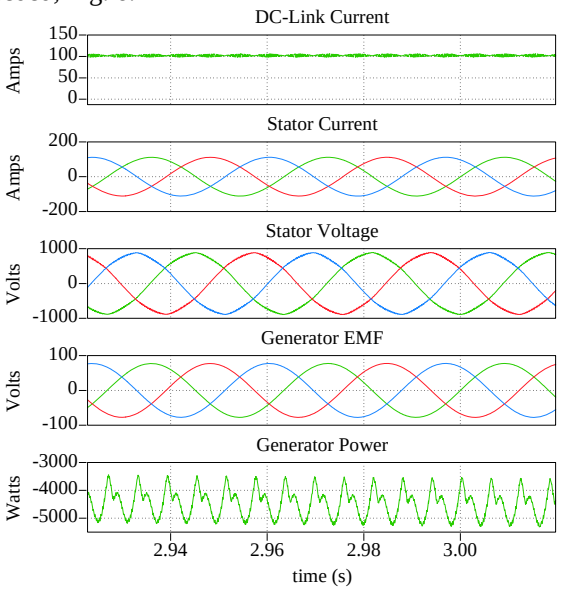

Fig. 3. CSC 200% rated load at 10kHz switching

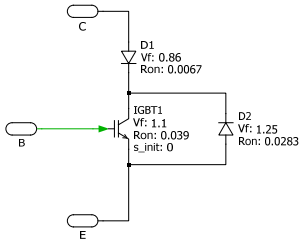

Fig. 4. PLECS® RB-IGBT model

A PLECS® RB-IGBT model has been created based upon the commercially available IRA37IH1200HJ module from IXYS, Fig. 4.

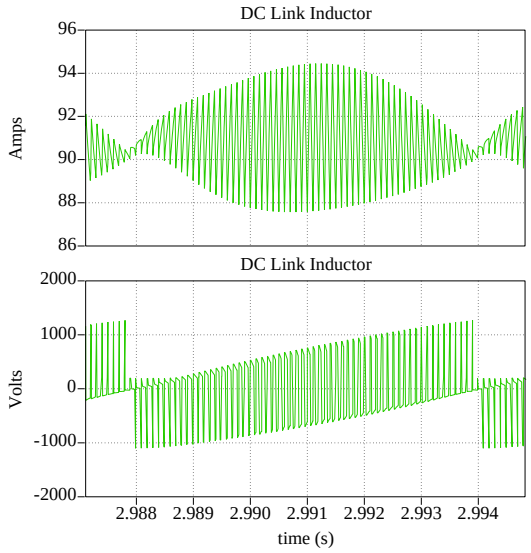

Fig. 5. CSC 200% load, 10kHz switching, 0.1mH DC link inductor

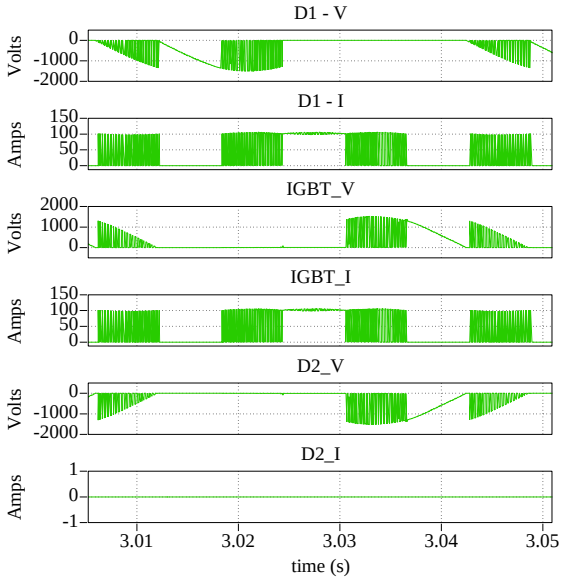

Fig. 6. CSC 200% load, 10kHz switching, example RB-IGBT waveforms

When delivering the maximum rated current of 50Apk at rated speed, the model predicts a healthy voltage margin for the switching devices. The existing model takes no account of reverse recovery, parasitic inductances or capacitances within the converter which will erode this margin in the prototype. Further development of the model to investigate the impacts of these issues will be necessary prior to prototype construction. This section concludes that the CSC with RB-IGBTs does have the potential to be used as a generator interface for a VHLM. There is some scope for optimising magnetic components within the generator, ESS or GIM at the same time as implementing the necessary PTO segment isolation, which is the subject of further investigation.

IV. WEC MODEL DEVELOPMENT

A. Problem analysis

A common approach to simulating the point absorber WEC is to use simplifying assumptions relating to the sea-state and device reaction: Sinusoidal monochromatic waves in deep water and limiting the degrees of motion to one axis only, i.e. heave. The buoy dimensions and motion are relatively small compared to the wavelength and wave height. The mass of the linear machine's translator is sufficient to keep the tether between the buoy and translator taut at all times, such that it can be assumed the buoy and generator are rigidly coupled together. Under these conditions the equation of motion, for the buoy without any generator force, can be represented by:

$$m\ddot{z} = A(\ddot{y} - \ddot{z}) + B(\dot{y} - \dot{z}) + C(y - z) \qquad (1)$$

Where: m is the buoy mass, A, B, C are the coefficients expressing the added mass, damping and hydrostatic stiffness, y is the vertical motion of the water surface and z is the vertical motion of the buoy.

One approach to analysing this problem is to represent the mechanical variables with their electrical equivalents [15]. In an electrical equivalent circuit, voltage represents force, current represents velocity, inductance represents mass, etc. Thus, an equivalent electrical circuit can be conceived and parameterised to represent the WEC operation as shown in Fig. 7. Here a voltage representing the applied force from the incoming wave, V_{fe}, is coupling with the buoy impedance and PTO impedance Z1 and Z2 respectively. Z1 is defined by the dimensions and mass of the selected buoy and might be considered to have a fixed value, whereas Z2 is adjustable by modifying the equations defining V_{fg} i.e. the generator force f_g. In reality, the parameters that make up Z1 are both frequency and magnitude dependant and are difficult to calculate for all but the simplest of buoys. Further, as the degree of motion in the buoy increases, non-linear effects will become more significant. For a specific buoy, these parameters can be more accurately identified either by experimental methods or computationally using tools such as WAMIT.

Under steady-state with linear operating conditions we can see how the maximum power capture might be predicted for a given excitation force. By controlling V_{fg} to adjust the generator impedance, Z2, to equal the complex conjugate of the WEC impedance, Z1, optimal power capture is achieved [10].

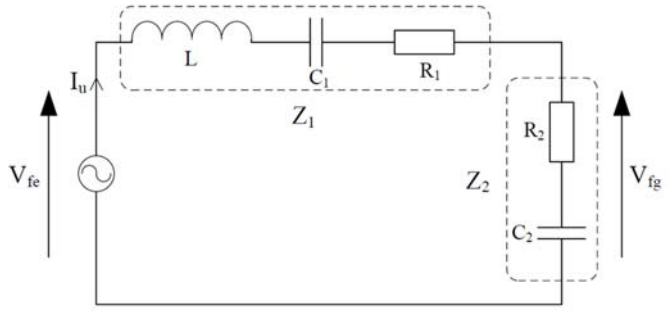

Fig. 7. Electrical equivalent circuit of the WEC

There are a number of problems with this model. Apart from the various second order hydrodynamic effects and the multi-dimensional motion, which we have chosen to ignore, significant non-linear events such as when the buoy exits the water or is fully submerged occur as a result of resonance or phase displacement. For maximum power capture, the point absorber is controlled to operate at or near its resonant frequency and as such the basic model is likely to predict unrealistic output power for a given buoy. Acknowledging the model is now operating outside of the original assumed conditions, it is still desirable to predict WEC general behaviour with some confidence, even if the accuracy is compromised. Three modifications to the basic model are proposed to address major non-linear events:

1. The buoy restoring force, $C(z)$, is proportional to the variation in position from equilibrium. However, should the buoy be fully submerged or leave the water, $C(z)$, is no longer be a simple linear function. In the model, $C(z)$ is held at a constant value outside of the linear region.
2. If the buoy leaves the water surface or is fully submerged, the wave excitation force $A(\ddot{y}) + B(\dot{y}) + C(y)$ is reduced to towards zero.
3. The linear machine's translator does not have infinite displacement. End spring forces have been introduced to prevent unrealistic translator excursions.

With these modifications in place the basic model ceases to predict wildly unrealistic motion when operating close to resonance.

B. Reactive power optimisation

However there is one further challenge to overcome, and that is the magnitude of reactive power that might be required to achieve resonant behaviour [10]. This reactive power is governed by the difference between the wave frequency and the natural resonant frequency of the WEC which is given by:

$$f_n = \frac{1}{2\pi}\sqrt{\frac{\rho g A_{wp} + k_s}{m + m_a}} \qquad (2)$$

Where: f_n is the natural frequency, ρ is the density of the fluid, A_{wp} is the water-plane area, $m + m_a$ is the mass and added mass of the buoy and k_s is the spring stiffness applied by the PTO, sometimes called reactive power. It can be seen that without reactive power the magnitude of the resonant frequency is related to the buoy water-plane area, A_{wp}, and inversely related to the mass of the buoy system and added mass of the displaced water, $m + m_a$. For a small point absorber there are a number of conflicting requirements when dimensioning the buoy. For example, assuming a simple cylindrical device:

1. The diameter of the buoy needs to be small in relation to the wavelength of the oncoming wave to be a point-absorber [16].
2. The draft of the buoy has an impact on the forces being applied by the wave. As buoy draft increases, the

inertial forces applied by the wave to the water-plane area diminish [17].

3. The buoy must be able to float.

Using wave data from South Uist [18], the most frequent wave has a significant wave height, Hs, of 2.75m and a period, T, of 7.25 seconds. Thus, a buoy with f_n centred at 0.138Hz would be well suited for this location. For E-Drive, taking the power in the wave and assuming a conversion efficiency, a cylinder with a diameter of 3m should produce an average output of 25kW in these seas. Unfortunately, even with a draft of 7m, f_n is 0.18Hz and such a large draft would severely affect the wave interaction [17]. For an ideal draft of around 2m, f_n is 0.3Hz.

One approach to achieve the desired resonant frequency is to modify the buoyancy restoring force, $\rho g A_{wp}$, with either springs or hydraulics. An alternative is to increase the effective mass of the buoy system by some means that does not adversely affect the wave interaction of the point absorber significantly. The Two Body system (TB-s) buoy demonstrated by Uppsala University is one option [17]. The upper body, the buoy, is optimised to capture the energy for the given wave regime and power requirements. The lower body is neutrally buoyant and held at sufficient depth to be unaffected by the surface waves. Provided the two tethers are always under tension, the lower body will act to increase m_a of the combined buoy system. The proposed arrangement is illustrated in Fig. 8. By increasing or decreasing the surface area of the lower body the natural frequency of the system can now be adjusted to achieve the desired f_n. The shape of the lower body can also be selected to optimise m_a whilst minimising any additional drag. A sphere is chosen for these initial investigations as the added mass is given by:

$$m_{as} = \frac{2}{3}\pi\rho r_s^3 \qquad (3)$$

Where: m_{as} is the added mass of the sphere and r_s is the radius of the sphere.

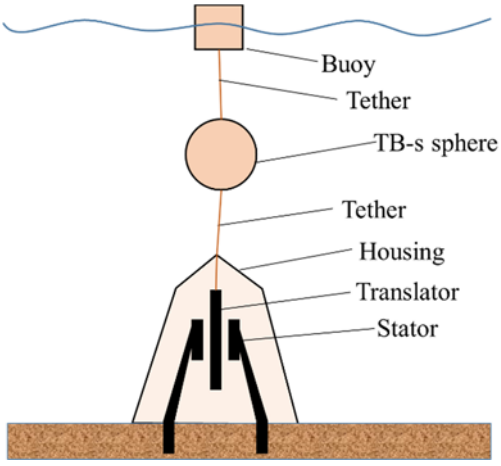

Fig. 8. General arrangement of point absorber buoy with TB-s sphere

An initial assessment of the TB-s sphere required for the E-Drive concept has been carried out by comparing f_n for a range of cylindrical buoys with a range of TB-s sphere diameters. Fig. 9 illustrates how the resonant frequency varies when adding a 4.4m diameter TB-s sphere over a wide range of buoy diameters and drafts. This particular sphere results in achieving the desired f_n of 0.14Hz when combined with a 3m diameter and 2m draft cylindrical buoy.

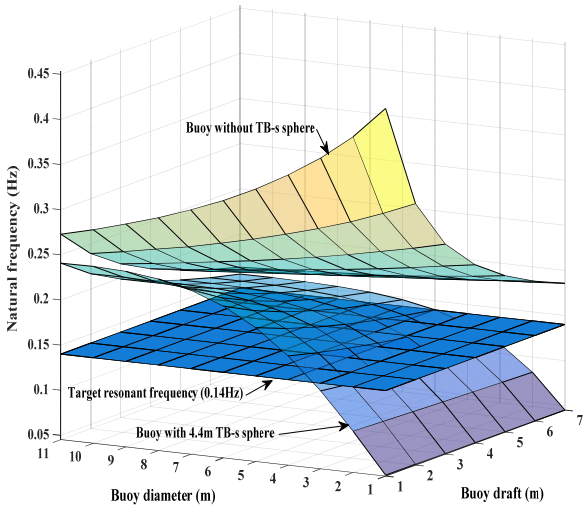

Fig. 9. Comparison of resonant frequency of point absorber buoy with and without TB-s sphere

C. *Model implementation using PLECS®*

To ensure a proper relationship between the buoy and wave position, the voltage representing the force on the buoy, $V_{fe,}$ is calculated using differentiators to determine $\ddot{y}, \dot{y}$ & y with the constants in (1), $A = M_w, B = B_w$ & $C = K_w$, being derived from the buoy and sphere geometry. The PLECS® implementation is shown in Fig. 10. Comparing the wave position and the buoy position allows determination of a non-linear event. Subsequent blocks modify V_{fe} accordingly. This approach provides confidence that the phase relationships between wave position and buoy motion are being estimated over a range of wave frequencies.

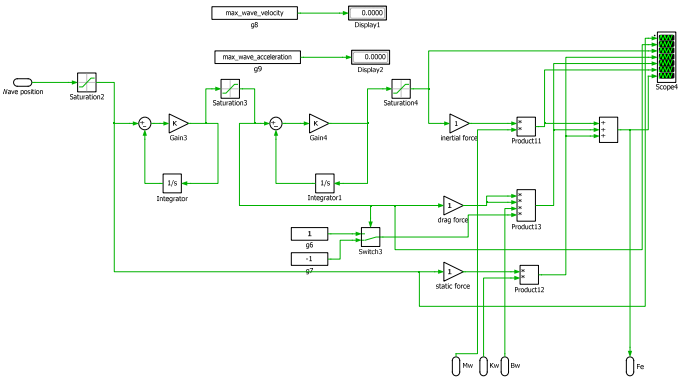

Fig. 10. Wave force calculations

The static buoy and TB-s constants for inertia, damping and spring force are all calculated based on classical methods as outlined in [1, 19]. Clearly there are limitations with this approach, but these force constants are easily calculated and

will give rise to general behaviour and order-of-magnitude predictions that can be validated by more sophisticated methods later.

The core of the model can be seen Fig. 11 with the buoy restoring force limit implemented with Zener diodes around the capacitor. This will clamp the capacitor voltage, i.e. the buoyancy force, when the buoy is fully submerged or out of the water, the maximum restoring force is a function of buoy geometry. Z_1 comprises the components RL1 and C3, the function blocks representing both the linear generator force and the end stop forces replace Z_2.

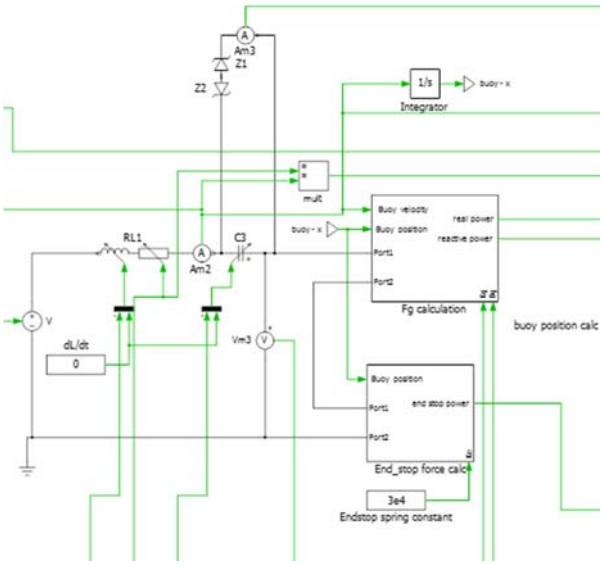

Fig. 11. Buoy and generator dynamic functions blocks

The values for K_g and B_g, which define the values of Z_2, are calculated to derive maximum power from the device using reactive power control under steady-state conditions [10]. i.e.:

$$B_g = B_w \quad (4)$$

$$\frac{K_g}{\omega} = \omega M - \frac{K_w}{\omega} \quad (5)$$

Where: B_g and B_w are generator and buoy damping coefficients respectively, K_g and K_w are generator and buoy restoring coefficients respectively and M is the combined mass and added mass of the system. The time varying generator force, f_g, is calculated as a function of buoy velocity and displacement.

V. RESULTS

A. *WEC Model predictions*

Example predictions from the WEC model for two sea-states are shown in Fig. 12. In the example, the WEC comprises a 3m diameter buoy with a 4.4m diameter neutrally buoyant TB-s sphere as described earlier. The combined mass of the generator translator and the buoy contributes to the draft of 2m. The available force from the generator has been limited in both the reactive, K_g and resistive B_g vectors to 44kN which is equivalent to the 100% load rating for the prototype generator.

In Fig. 12(a) the applied sea-state is coincidental with the WEC resonant frequency of 0.14Hz. The required mechanical reactive power is minimal and the average power extracted is close to the total generator power of 20kVA. Note, this generator reactive power is an electrical equivalent to the actual mechanical force (V) multiplied by velocity (A) being represented in the model. No account of generator conversion efficiency or converter efficiency is incorporated at this stage.

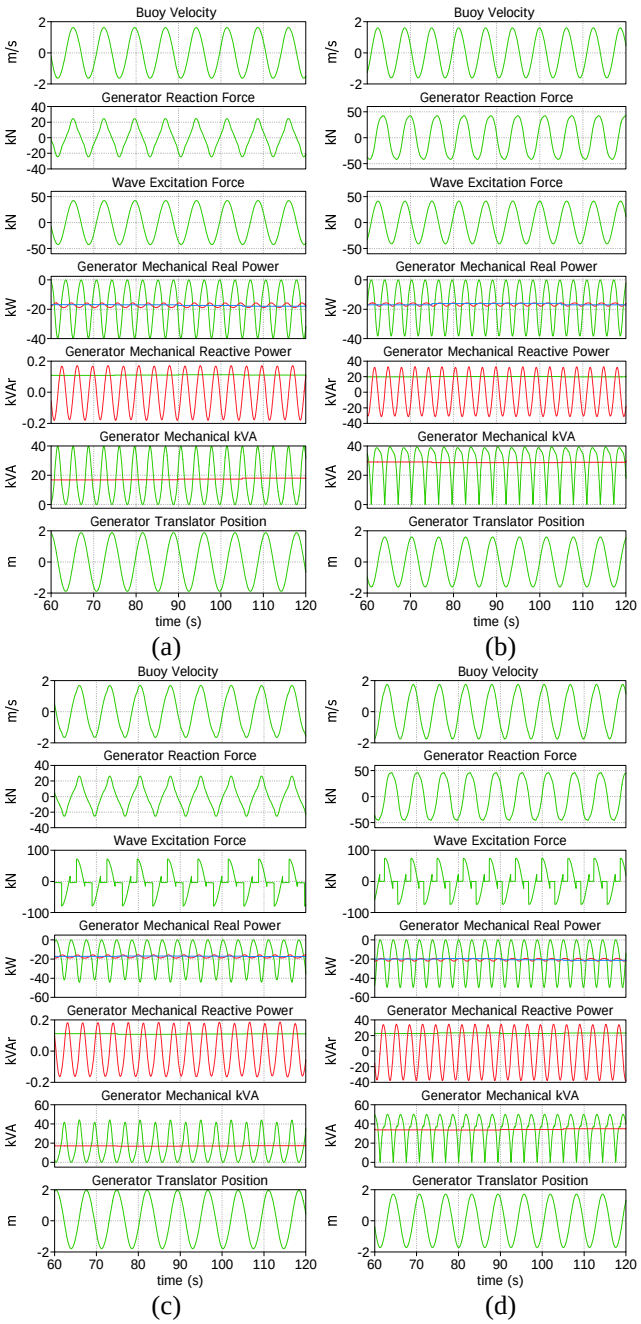

Fig. 12. WEC model predictions with reactive power control under multiple sea-states: (a) Hs = 1.25m, T = 7.25s (b) Hs = 1.25, T= 6.25s c(a) Hs = 2.25m, T = 7.25s (d) Hs = 2.25, T= 6.25s

In Fig. 12(b), a shorter period sea-state is applied to the buoy to which the model is now predicting an increased average

power flow of 21kW but at a cost of an additional 20kVAr to tune the device. The generator kVA demand has increased to around 30kVA in this case. In Fig. 12(c) & (d), where the amplitude of the sea-state has increased to Hs = 2.25m, the buoy resonance exhibits excessive motion, resulting in discontinuities. When the buoy is predicted to be leaving the water or being fully submerged, the model compensates by clamping the wave excitation. As a result, the predicted power output from the buoy and reactive power demand are little changed even though Hs is much larger, i.e. the conversion efficiency of the WEC has been reduced.

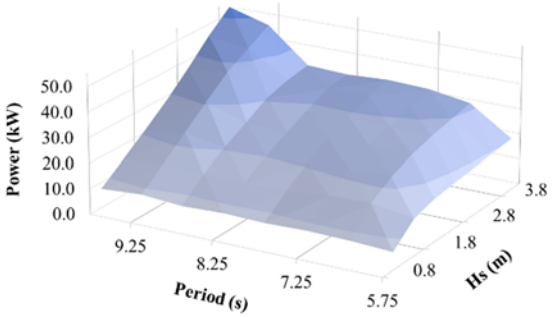

Fig. 13. Average mechanical power for a range of sea-states.

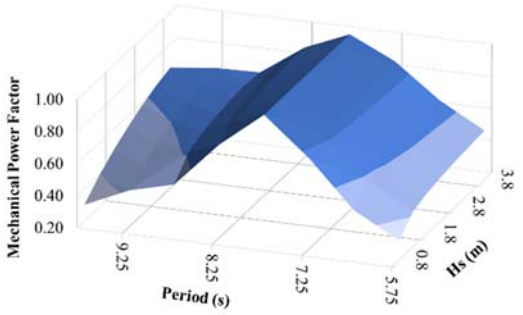

Fig. 14. Mechanical power factor for a range of sea-states

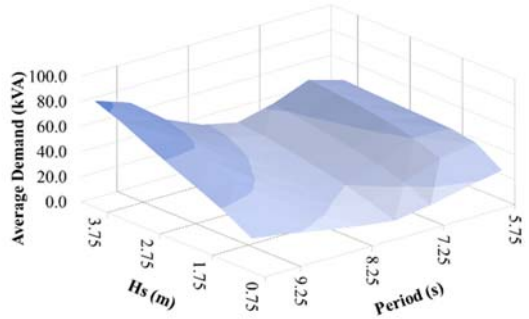

Fig. 15. Average mechanical kVA demand from the generator for range of sea-states.

Acknowledging that this simplified model requires further validation, which is ongoing within the project, it is now predicting the magnitude and general form of the mechanical power required from the generator over a range of simulated monochromatic sea-states. It is, therefore, a straightforward task to run the model over a wider range of sea-states to capture the mechanical output power, mechanical power factor and equivalent mechanical kVA capacity required for the generator. Examples are presented in Fig. 13, Fig. 14 & Fig. 15.

The advantage of this modelling approach is that we can couple the WEC model directly to CSC model to further investigate the dynamic operation and control of the PTO.

B. WEC model coupled to CSC

The CSC is configured to control the DC-link current directly from, f_g, which is calculated by the WEC model. The VHLM control within the CSC is configured such that the phase current is always in-phase or 180 degrees out-of-phase with the back-emf, the force applied by the translator is bidirectional and the converter is fully four-quadrant.

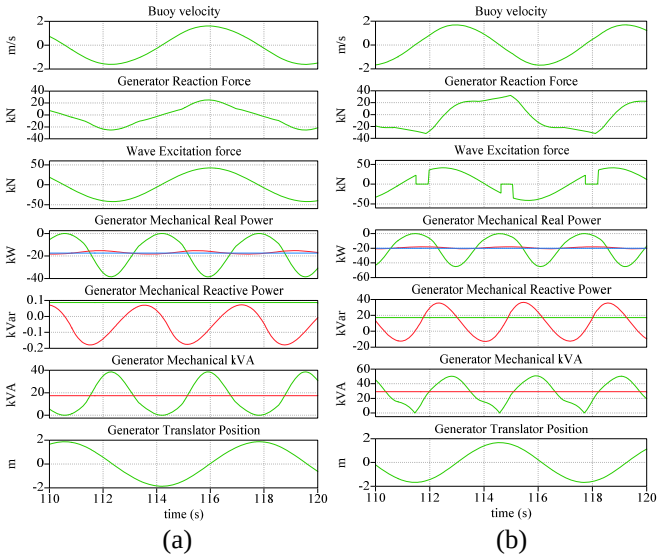

Fig. 16. WEC conditions for CSC demonstration (a) Hs = 1.25m, T=7.25s and (b) Hs = 1.25m, T=6.25s

For the CSC results shown in Fig. 16 & Fig. 17, the model is operated with Hs =1.25m and the period, T, is altered between 6.25 and 7.25seconds. The average mechanical power is constant at approx. 20kW. In Fig. 16 the expanded view illustrates the generator force demand and power flux as additional mechanical reactive power is required for tuning the WEC as T=6.25s. Also, the generator needs to be capable of providing significant force even at zero velocity with reactive force control.

For this initial demonstration of the E-drive 25kW PTO, it is envisaged that the complete VLHM linear generator would comprise ten individual 2.5kW segments, each with their own CSC. The VHLM in the model has a power factor of 0.2 and efficiency of 0.9, typical values for a VHLM design [20]. The CSC waveforms for the time period depicted in Fig. 16 are shown below in Fig. 17. The impact of the generator efficiency and low power factor on converter kVA rating are clearly demonstrated here. The segment CSC rating is around 7kVA

for average output power of 2.5kW at T=7.25s increasing to 8kVA for an average output power of 1kW at T=6.25s. The energy storage requirements are predicted by integrating the difference between input power and the average output power from the CSC. The pk-pk storage requirements increase with reactive power control from 3.22kJ at T=7.25s to 4.15kJ at T=6.25s .

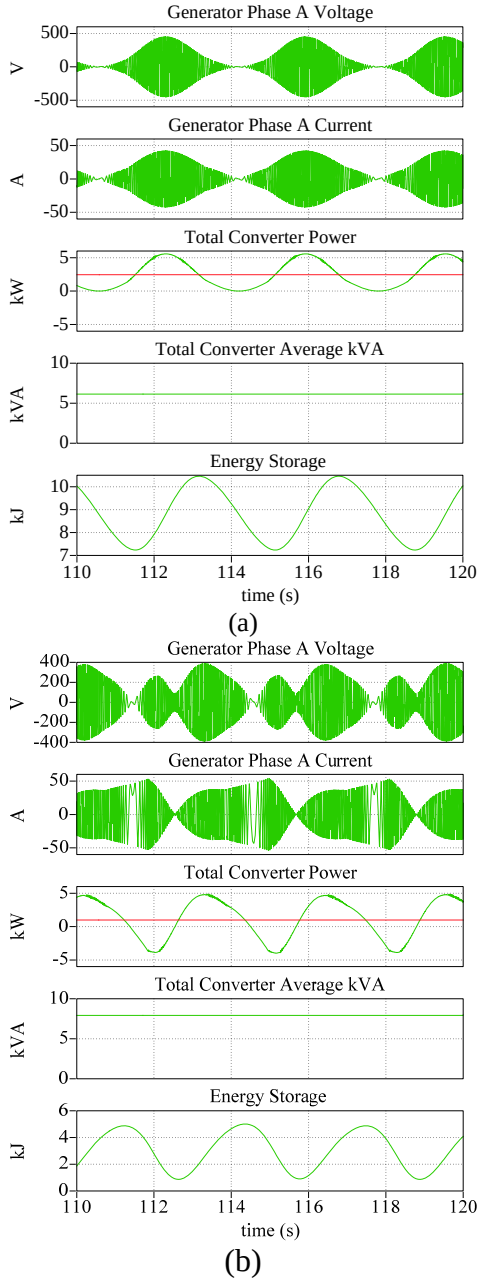

Fig. 17. Predicted waveforms from one PTO CSC and generator segment. (a) Hs = 1.25m, T=7.25s and (b) Hs = 1.25m, T=6.25s

The WEC model and CSC predictions can predict a wide range of WEC operating conditions and support further investigation into the CSC and generator. In this example the translator velocity and force demands from the WEC are matched to the continuous ratings of this particular generator, but a wider range of sea-states requires investigation as do confused seas.

VI. Discussion

A. *Energy storage within the direct drive system*

Cost effective and reliable energy storage is considered a vital element for a direct-drive PTO. Power density and the energy density, KWh/kg and kW/kg, are typically used for comparison between storage devices. In the WEC it could be argued weight is less of an issue and volume is perhaps more relevant for a device mounted PTO. An initial comparison based on readily available data for various capacitors and a DC-link inductor is presented in Table 1. It appears that the inductor is nowhere near as effective as either the electrolytic or film capacitor in terms of energy density or power density. The Ultra-capacitor, provided it can meet the reliability requirements, is the obvious contender for levelling the mechanical and reactive power flows through the CSC.

Perhaps a better designed DC-link inductor will offer equal benefits in terms of power density as the electrolytic capacitors and the reliability should be higher, but this initial investigation suggests caution is required when carrying out a side by side comparison between the CSC and a VSC if DC-link energy storage is a key criteria. Any capacitor based ESS can only be effective if the terminal voltage can vary freely; a suitable interface for the CSC will be investigated.

Where there is significant room for optimisation for the CSC is in combining the DC-Link inductor with other essential electromagnetic components and perhaps incorporating it within the generator itself. This will be an avenue of ongoing investigation.

Table 1 – Energy storage comparisons

	Electrolytic Capacitor 450V [21]	**Film Capacitor 450V [21]**	**DC inductor [22]**	**Ultra-capacitor [23]**
Energy density (j/m^3)	$6.53x10^5$	$1.04x10^5$	$6.94x10^2$	$5.4x10^7$
Power density (w/m^3)	$1.85x10^7$	$9.07x10^7$	$3.92x10^3$ ($3.9x10^5$)*	$3.6x10^5$

*Power density achievable with 100% Pk-Pk current ripple

B. *CSC development*

The CSC requires a capacitor commutation filter on the generator interface. During investigations it was identified as a potential source of resonance and care is required to avoid machine harmonics or fundamental frequencies from exciting these. Techniques do exist to mitigate such resonances [14].

The CSC is traditionally a solution for high power drives with switching devices operating at low frequencies. Higher frequency switching devices appear to offer benefits in terms of reduced DC-Link and filter sizes, but it is yet to be seen if the parasitic inductances and blocking diode reverse recovery are problematic. Finally, the metrics of merit for this particular

PTO approach should be compared with conventional solutions and will be a matter of interest.

Significant over-speed or overload conditions for the VLHM generator need to be fully quantified at the system design stage as the high stator inductance will quickly result in dangerous overvoltage situations building up for the converter should they occur. Additionally, should the converter fail, the generator will continue to produce voltages if the WEC is allowed the freedom to move. Unchecked it could interact with the filter capacitors resulting in excessive terminal voltages.

VII. Conclusion

The current status of a project to develop key elements of a WEC direct-drive PTO have been described here. Simulation methods have been used to demonstrate the feasibility of providing four-quadrant control of a VHLM being operated as a linear generator within a WEC with a CSC. It is clear that the inherent low power factor of the VHLM when combined with the mechanical reactive power requirements of the WEC can create problems for the CSC designer in terms of increasing the overall kVA requirements and potential overload.

The time domain WEC model when coupled to the CSC provides interesting insight into the dimensional requirements for the PTO as a whole. The next step for this work is to compare our basic model with a full wave to wire model being developed by the by project partners using WAMIT.

The E-Drive project is still at a relatively early stage and a number of design issues remain to be addressed. Detailed design of prototype CSC hardware and investigations into the other key elements of the PTO will be carried out over the next year.

Acknowledgment

This work has been funded by EPSRC Ref. EP/N021452/1, All Electrical Drive Train for Marine Energy Converters (EDRIVE-MEC) under SUPERGEN Marine 2015.

References

[1] M. E. McCormick, *Ocean Wave Energy Conversion*. New York: Dover Publications, Inc., 2007.

[2] E. Tedeschi, M. Molinas, M. Carraro, and P. Mattavelli, "Analysis of power extraction from irregular waves by all-electric power take off," in *2010 IEEE Energy Conversion Congress and Exposition*, 2010, pp. 2370-2377.

[3] J. K. H. Shek, D. E. Macpherson, and M. A. Mueller, "Power conversion for wave energy applications," in *Power Electronics, Machines and Drives (PEMD 2010), 5th IET International Conference on*, 2010, pp. 1-6.

[4] D. Bould. (2016, 2/1/2017). *e-Drive: All Electrical Drive Train for Marine Energy Converters* Available: http://www.edrive.eng.ed.ac.uk/

[5] N.J.Baker, M.A.Mueller, and M.A.H.Raihan, "All electric drive train for wave energy power take off " presented at the IET Conference on Renewable Power Generation, London, 2016.

[6] J. Sjolte, G. Tjensvoll, and M. Molinas, "All-electric Wave Energy Converter array with energy storage and reactive power compensation for improved power quality," in *2012 IEEE Energy Conversion Congress and Exposition (ECCE)*, 2012, pp. 954-961.

[7] M. Alberdi, M. Amundarain, A. J. Garrido, I. Garrido, and F. J. Maseda, "Fault-Ride-Through Capability of Oscillating-Water-Column-Based Wave-Power-Generation Plants Equipped With Doubly Fed Induction Generator and Airflow Control," *IEEE Transactions on Industrial Electronics*, vol. 58, pp. 1501-1517, 2011.

[8] D. B. Murray, J. G. Hayes, M. G. Egan, and D. L. O. Sullivan, "Supercapacitor testing for power smoothing in a variable speed offshore Wave Energy Converter," in *2011 Twenty-Sixth Annual IEEE Applied Power Electronics Conference and Exposition (APEC)*, 2011, pp. 1933-1939.

[9] G. Brando, A. Dannier, A. D. Pizzo, L. P. D. Noia, and C. Pisani, "Grid connection of wave energy converter in heaving mode operation by supercapacitor storage technology," *IET Renewable Power Generation*, vol. 10, pp. 88-97, 2016.

[10] J. K. H. Shek, D. E. Macpherson, M. A. Mueller, and J. Xiang, "Reaction force control of a linear electrical generator for direct drive wave energy conversion," *IET Renewable Power Generation*, vol. 1, pp. 17-24, 2007.

[11] T. Soong and P. W. Lehn, "Assessment of Fault Tolerance in Modular Multilevel Converters With Integrated Energy Storage," *IEEE Transactions on Power Electronics*, vol. 31, pp. 4085-4095, 2016.

[12] H. Wang, M. Liserre, and F. Blaabjerg, "Toward Reliable Power Electronics: Challenges, Design Tools, and Opportunities," *IEEE Industrial Electronics Magazine*, vol. 7, pp. 17-26, 2013.

[13] A. De, S. Roy, and S. Bhattacharya, "Comparative suitability evaluation of reverse-blocking IGBTs for current-source based converter," in *2014 International Power Electronics Conference (IPEC-Hiroshima 2014 - ECCE ASIA)*, 2014, pp. 2562-2568.

[14] W. Bin, "High-Power Converters and AC Drives," in *High-Power Converters and AC Drives*, ed: Wiley-IEEE Press, 2006, pp. 1-333.

[15] G. Thomas, "Dimensional analysis applied to electricity and mechanics," *Physics Education*, vol. 14, p. 116, 1979.

[16] J. Falnes, *Ocean Waves and Oscillating Systems*. New York: Cambridge University Press, 2002.

[17] J. Engström, M. Eriksson, J. Isberg, and M. Leijon, "Wave energy converter with enhanced amplitude response at frequencies coinciding with Swedish west coast sea states by use of a supplementary submerged body," *Journal of Applied Physics*, vol. 106, p. 064512, 2009.

[18] R. H. Bracewell, "FROG and PS FROG: A study of two reactionless ocean wave energy converters," PhD Thesis, Lancaster University, 1990.

[19] M. H. Patel, *Dynamics of Offshore Structures*. London: Butterworths & Co., 1989.

[20] E. Spooner and L. Haydock, "Vernier hybrid machines," *IEE Proceedings - Electric Power Applications*, vol. 150, pp. 655-662, 2003.

[21] M. Salcone and J. Bond, "Selecting film bus link capacitors for high performance inverter applications," in *2009 IEEE International Electric Machines and Drives Conference*, 2009, pp. 1692-1699.

[22] W. Walcott, "DCA Link Chokes - User Manual," Rev 001, INSTR - 021 REL. 060612 ed: MTE Corperation, 2006.

[23] Z. S. Wu, K. Parvez, X. Feng, and K. Müllen, "Graphene-based in-plane micro-supercapacitors with high power and energy densities," *Nature Communications*, vol. 4, p. 2487, 09/17/online 2013.